# Hydrological conditions control dissolved organic matter dynamics along a peatland headwater boreal stream

**Antonin Prijac[1,2,3], Laure Gandois[4], Pierre Taillardat[1,5], Michelle Garneau[1,2,3,6]**

[1] Centre de Recherche sur la Dynamique du Système Terre (GÉOTOP), Université du Québec à Montréal, Montréal, Canada
[2] Groupe de Recherche Interuniversitaire en limnologie (GRIL), Université du Québec à Montréal, Montréal, Canada
[3] Institut des Sciences de l'Environnement (ISE), Université du Québec à Montréal, Montréal, Canada
[4] Laboratoire Écologie Fonctionnelle et Environnement, UMR 5245, CNRS-UPS-INPT, Toulouse, France
[5]NUS Environmental Research Institute, National University of Singapore, Singapore
[6] Département de Géographie, Université du Québec à Montréal, Montréal, Canada

**Corresponding authors:** Antonin Prijac (prijac.antonin@uqam.ca) and Laure Gandois (laure.gandois@cnrs.fr)

## Abstract

Hydrological conditions (i.e., high-flow versus low-flow) in peatland drainage streams influence both the quantity of dissolved organic carbon (DOC) exports and dissolved organic matter (DOM) composition. Yet, our knowledge on DOM fate after exports from the peatland remains limited while this highly reactive component sustains emissions and exports of carbon dioxide ($CO_2$) from streams through degradation processes. The present study demonstrates the relationships between DOM composition evolution and catchment hydrological conditions along a 3 km long headwater stream running through a boreal peatland, from its source to the outlet. Our results show that hydrological conditions significantly influenced DOM composition evolution along the stream. DOM exported during high-flow conditions presented a composition similar to peat porewater in terms of DOC:DON ratio and aromaticity, but a lower average molecular weight, indicating preferential exports of low molecular weight DOM recently produced in the acrotelm. The DOM composition changed little along the stream during high-flow as it was rapidly flushed downstream. During low-flow conditions, DOM composition evolved along the stream in contrast to high-flow with a strong increase in DOM aromaticity and molecular weight along the stream. These changes were significantly correlated to the water residence time in the stream and to the estimated proportion of mineralized DOC to total DOC

flux exported at the stream outlet. These results highlight the importance of hydrological conditions on DOM dynamics as DOM was locally mineralized during low-flow conditions, when DOC exports were low, while mineralization processes happened downstream under high-flow conditions which favored important DOC exports.

## 1. Introduction

Among terrestrial ecosystems, peatlands play a crucial role in the carbon cycle as they represent an important carbon sink, as a result of accumulating organic carbon fixed by its vegetation under the form of peat (Charman, 2002; Yu et al., 2010). It was also established that, at the catchment scale, the amount of carbon exported as dissolved organic carbon (DOC) is positively correlated to the proportion of the catchment area covered by peatlands (Billett et al., 2006; Laudon et al., 2011; Olefeldt et al., 2013; Rantakari et al., 2010). DOC is the main form of carbon being laterally exported from peatland ecosystems, accounting from 57 % to 97 % of aquatic carbon fluxes (Dinsmore et al., 2010, 2013; Holden et al., 2012; Leach et al., 2016; Roulet et al., 2007). The remaining part is constituted by particulate organic carbon (POC), dissolved carbon dioxide ($CO_2$) and methane ($CH_4$). Moreover, several studies have shown that DOC export from peatland can offset 14-132 % of its net ecosystem exchange (Dinsmore et al., 2010; Nilsson et al., 2008; Roulet et al., 2007; Worrall et al., 2008), even exceeding the net ecosystem exchange for some years (Koehler et al., 2011; Roulet et al., 2007).

The aquatic DOC export through peatland drainage streams is highly sensitive to hydrological conditions in catchments, and mainly in peatland areas. The rise of peatland water table depth (WTD) leads to the increase of hydrological connectivity between peatland and stream and facilitates DOC transfer through subsurface flow during flood periods (Birkel et al., 2017; Bishop et al., 2004; Frei et al., 2010; Laudon et al., 2011; Tunaley et al., 2016). Additionally to the importance of DOC in aquatic carbon exports, it is necessary to evaluate if this form of carbon is reactive and can be mineralized through biodegradation and photodegradation processes in streams (Lapierre & del Giorgio, 2014; Vonk et al., 2015), to fully understand its fate – either mineralized as $CO_2$ and sent back to the atmosphere or transported downstream. In headwater streams, dissolved organic matter (DOM) mineralization leads to $CO_2$

production (Hutchins et al., 2017; Rasilo et al., 2017) hence generating emissions of $CO_2$ from headwater streams (Taillardat et al., 2022; Wallin et al., 2013).

Several studies previously explored the evolution of DOM composition along river transects (i.e., from its source to its outlet within a catchment) through the optical or molecular properties, or assessments of biodegradability. These studies aimed at demonstrating the influence of land use change (Hope et al., 1997; Kamjunke et al., 2019; Miller, 2012; Yamashita et al., 2010), dams and reservoirs (Parks & Baker, 1997; Stackpoole et al., 2014; Zurbrügg et al., 2013) on DOM composition evolution in streams and rivers. The respective influence of multiple DOM sources and tributaries contributions within large river catchments were also assessed using this approach (Cawley et al., 2012; del Giorgio & Pace, 2008; Frederick et al., 2012; Lambert et al., 2016; Mladenov et al., 2007; N. D. Ward et al., 2015). These studies focused on catchments with surface areas ranging from 5,500 $km^2$ (Yamashita et al., 2010) or larger (i.e., up to 1,353,000 $km^2$ in Stackpoole et al., 2014).

Consequently, Raymond et al. (2016) proposed the *pulse-shunt* concept to conceptualize the fate of DOC exported through streams and rivers networks. While Cole et al. (2007) described rivers as a reactor rather than the common acceptance of them as passive pipes, Raymond et al. (2016) hypothesized that streams can be one or the other depending on hydrological connectivity between terrestrial ecosystems (e.g., peatlands) and rivers. After precipitation or during snowmelt, important discharge and short residence times induce large mobilization of DOM through rivers leading to the passive transfer of DOM up to coastal ecosystems. Elsewhere, periods of low hydrological connectivity led to lower DOM exports. The lower discharge and longer residence time during these periods enhance DOM mineralization in streams that sustains $CO_2$ exports and emissions.

Effects of hydrological connectivity on DOM mineralization at smaller scales and especially headwater stream catchments are less documented. Headwater streams are recognized to be molecularly more diversified compared to downstream rivers (Kamjunke et al., 2019; Lambert et al., 2016; Vannote et al., 1980; N. D. Ward et al., 2015; Zark & Dittmar, 2018), induced by the simultaneous contribution of allochthonous DOM derived terrestrial environments (e.g., peatlands) and autochthonous DOM production from biodegradation and photodegradation processes (Berggren et al., 2010; Mann et al., 2015; Vonk et al., 2015).

Therefore, mineralization processes can be identified by using DOM composition evolution (Grand-Clement et al., 2014; Payandi-Rolland et al., 2020; Prijac et al., 2022). Low molecular weight compounds are preferentially degraded by microorganisms (Mann et al., 2015; Spencer et al., 2008, 2015; Worrall et al., 2017), with a subsequent increase in aromaticity and molecular weight for the remaining DOM (Autio et al., 2016; Hulatt et al., 2014; Prijac et al., 2022). Conversely, photodegradation degrades aromatic compounds (Cory et al., 2007, 2013), and therefore decreases DOM molecular weight and aromaticity of stream DOM (Helms et al., 2008; Laurion & Mladenov, 2013; C. P. Ward & Cory, 2016). In addition to mineralization processes, stream DOM composition can vary according to its vertical stratification of DOM composition in contributing peat layers. This stratification is induced by WTD fluctuations, as well as impact on microbial and plant metabolism (Broder & Biester, 2015; Buzek et al., 2019; Tfaily et al., 2013, 2018) leading to an increase of DOM aromaticity and molecular weight with depth (Tfaily et al., 2018).

In peatland-dominated headwater catchments, previous studies have explored changes in DOM composition by comparing different hydrological conditions (i.e., periods of low- and high-flow in the stream) or during different seasons (Austnes et al., 2010; Broder et al., 2017; Buzek et al., 2019; Grand-Clement et al., 2014). However, these studies only considered one sampling station in a stream and commonly selected the outlet of catchments (Austnes et al., 2010; Broder et al., 2017; Buzek et al., 2019) or compared distinct catchments according to their land cover (Grand-Clement et al., 2014). Despite these studies observed shift in DOM composition from recently produced DOM from the acrotelm during high-flow (Austnes et al., 2010) to more microbial-derived DOM during low-flow (Grand-Clement et al., 2014; Hutchins et al., 2017) they did not explore the change along a stream transect (i.e., from its source to its outlet).

The goal of this study is to understand the effect of hydrological conditions on DOM composition in a stream running through a boreal peatland-dominated catchment. While the *pulse-shunt* concept focused on variation of DOM exports under contrasted hydrological condition in stream, here we hypothesized that for a peatland-dominated headwater catchment, DOM composition evolution is also influenced by hydrological conditions. While it commonly assumed that mineralization processes affect DOM composition, the contribution of the study

would identify if and how residence time, under contrasted hydrological conditions, could affect mineralization processes magnitude and consequently the DOM composition. More specifically, the study aims at i) comparing DOM composition in the stream and in the peat porewater under different hydroclimatic conditions and ii) describing the spatiotemporal variability of DOM composition under the different hydroclimatic conditions along a stream transect. The study combines investigations of DOM composition at different sampling stations along a 3 km long stream transect, and present punctual mass balance models under different hydrometeorological conditions (consisting of high-flow and low-flow conditions) to estimate peatland contribution of DOC exports.

## 2. Study site

The study site, within the Romaine River catchment (14 500 $km^2$) is located in north-eastern Canada, was previously described (Prijac et al., 2022, 2023; Taillardat et al., 2022). The site is in the eastern spruce-moss bioclimatic domain of the closed boreal forest (Payette, 2001) at the limit of the coastal plain and the Highlands of the Laurentian Plateau of the Precambrian Shield (Dubois, 1980). The studied catchment is covered at 76% by the Bouleau peatland (50°31'N, 63°12'W; alt: 108 ± 5 m), an ombrotrophic slightly dome-shaped bog (Fig. 1). Peat accumulation was initiated at ca 9260 calibrated years before present and maximum peat depth reaches 440 cm (Primeau & Garneau, 2021). The peatland is positioned at the head of a catchment and the study focussed on the southern section of the peatland drained by a headwater stream of 3 km long, which is flowing from North to South predominantly on the western side of the peatland. The surface of the catchment drained by the stream is 2.22 $km^2$ and is covered at 76.7 % by peat, representing a surface area of 1.70 $km^2$.

As previously described (Prijac et al., 2022, 2023; Taillardat et al., 2022) the regional climate data give a mean annual temperature of 1.5°C and mean annual precipitation of 1011 mm of which 590 mm fall as snow. Average monthly positive temperature occurs from May to October with 1915 growing degree days above zero (Havre-Saint-Pierre meteorological station, mean 1990-2019, Environment of Canada). Over the growing seasons, average air temperature was 13.2 ± 6.9°C with a minimum temperature of -7.9°C in early October 2018 and a maximum of 30.8°C reached in late July 2018. Average precipitation events were 2 mm $h^{-1}$ and maximum

precipitation fallen in one hour was in July 2018 with a total of 22 mm. The wettest month was August 2018 with a total precipitation of 207 mm and the driest month July 2018 with a total precipitation of 27 mm.

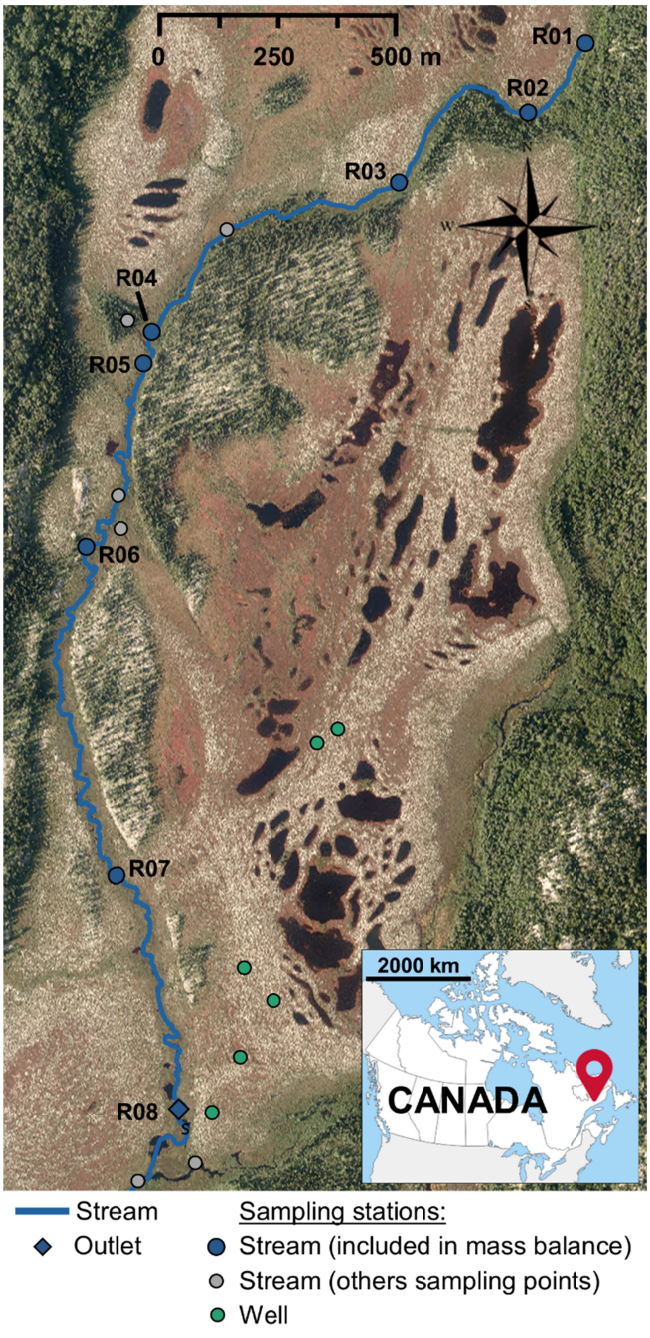


**Figure 1.** Bouleau peatland with the location of the

sampling sites in wells (green dots), pools (yellow triangles) and in the stream (blue dots) and its tributaries (grey dots). The aerial photo was provided by Hydro-Québec.

153

154 # 3. Material and methods

155 ## 3.1 Water sampling

156 The water sampling was performed four times during the growing season of 2019 (June,
157 August, September, and October). Following the method described in Prijac et al. (2022, 2023),
158 the water was sampled at the surface of eight stations along the headwater stream and peat
159 porewater was sampled from six wells (P1 to P6, Fig. 1) located along a topographic gradient
160 from the peatland dome (higher elevation) to its southern edge, near the stream outlet (lower
161 elevation). The peat porewater was collected into two meters long PVC wells, perforated,
162 covered with a nylon sock to avoid infilling by peat and inserted in peat to collect water from the
163 first two meters of the peat column.

164 Physicochemical parameters (temperature, pH, specific conductivity, and dissolved
165 oxygen saturation) were measured at each sampling site using a multi-parameter portable meter
166 (Multiline Multi-3620 IDS, WTW, Germany) calibrated before each field visit. Water samples
167 were collected in clean polypropylene (PP) bottles (acid rinsed) and filtered on pre-combusted
168 (4h at 450°C) GF/F filters (Whatman).

169 ## 3.2 DOM analyses

170 ### 3.2.1 DOC and DON concentrations

171 Following the method described in Prijac et al. (2022), the filtered water samples were
172 prepared for DOC and total nitrogen (TN) analyses by acidification to pH 2 with 1M HCl and
173 stored in 40 mL glass vials. The DOC and TN concentrations were analyzed using the catalytic
174 oxidation method followed by non-dispersive infrared (NDIR) detection of $CO_2$ produced (TOC

analyser TOC-L, Shimadzu, Japan) with limits of quantification of 0.1 mg C $L^{-1}$ and 0.2 mg N $L^{-1}$. The samples were prepared for cation and anion analyses and stored in high-density polyethylene (HDPE) vials without acidification. These ions (chloride, ammonium, nitrites, and nitrates) were analyzed by high performance liquid chromatography (HPLC) coupled with a Dionex ICS-5000+ analyzer for anions (Thermo Fisher Scientific) and a Dionex DX-120 analyzer for cations (Thermo Fisher Scientific). The reference materials included ION-915 and ION 96.4 (Environment and Climate Change Canada, Canada). Analyses were performed at Laboratoire Ecologie fonctionnelle et environnement (UMR 5245 CNRS – UT3 – INPT, France). Dissolved organic nitrogen (DON) corresponds to the difference between the concentration of TN and the sum of concentration of inorganic nitrogen (ammonium, nitrites, and nitrates).

### 3.2.2 Stable isotopic analyses

Analyses of $\delta^{13}$C-DOC were realized at the Jan Veizer stable isotope laboratory (University of Ottawa, Canada) following the method described in Prijac et al. (2022) and developed by Lalonde et al. (2014). The samples were acidified to pH 2 with 1M HCl and stored in 40 mL quality certified ultra-clean borosilicate glass vials. The first step involved catalytic oxidation of DOC followed by a solid-state non-dispersive infrared (SS-NDIR) detection of the $CO_2$ produced (OI Aurora 1030C, Xylem Analytics, USA). The $CO_2$ produced was passed through a chemical trap and a Nafion trap prior to $^{13}$C isotopic analyses using isotope-ratio mass spectroscopy (IRMS, Thermo Finnigan DeltaPlus XP, Thermo Electron Corporation, USA). The results were standardized with organic standards (KHP and sucrose) and $^{13}C/^{12}C$ ratios were expressed as per mil deviations from the international standard VPDB.

### 3.2.3 Optical analyses

As in Prijac et al. (2022), UV-visible analyses were performed on samples filtered on GF/F filters and absorbance was measured from 180 to 900 nm with a 5 nm resolution.

Absorbance analyses were performed on ) Duetta (Horiba, Japan) over a wavelength range from 190 to 900 nm at 2 nm intervals. All analyses were realized at the Groupe de recherche interuniversitaire en limnologie (GRIL, UQAM, Canada).

The absorbance indices were calculated to provide information about DOM composition. These indices were $SUVA_{254}$ (L $mg^{-1}$ $m^{-1}$) which is a proxy of the DOM's aromatic content, calculated and corrected to ferric iron interaction following the method described in Weishaar et al. (2003), $E2$ : $E3$ ratio, and spectral slope ratio ($S_R$) which are proxies of the average DOM molecular weight (Haan & Boer, 1987; Helms et al., 2008).

Spectrofluorometric analyses were also conducted on Duetta (Horiba, Japan) at the GRIL laboratory. Samples were excited at a range from 230 to 450 nm (at 2 nm resolution) and fluorescence was measured at a range from 240 to 600 nm (at a 5 nm resolution). Prior to the analyses, samples were diluted when necessary to maintain an absorbance intensity at 254 nm below 0.6 and avoid inner filter effect. A blank sample with MilliQ water (Merck-Millipore, Germany) was measured prior to sample analyses. Samples spectra were obtained by subtracting the blank spectra to eliminate the Raman scatter peak. The operation was conducted automatically by the analytical equipment.

### 3.3 Incubation experiments for the determination of the proportion on mineralized DOC into the DOC exports

Incubation experiments were performed during three sampling periods in 2019, from 7 to 13 June, from 31 July to 7 August, and from 4 to 10 September. Samples were collected at the stream outlet where water temperature was monitored using an EXO2 probe (YSI, USA).

Incubation experiments followed the method described in Prijac et al. (2022) with samples filtered on GF/F filters (Whatman). Samples were placed on amber glass to test biodegradation (BIO) only and in transparent vials to test both bio and photodegradation (BIO+PHOTO). For *in situ* incubations (IS), the samples were placed 1-2 cm below the water surface at the outlet of the peatland (Fig. 1). For controlled conditions (CC), vials were placed in a dark room in a laboratory space near the study site (Havre-Saint-Pierre) where the temperature was maintained between 18 and 20°C and controlled twice each day. Both *in situ* and controlled conditions started the same day.

In the end, samples incubated under UF conditions (n = 27) and filtered on a GF/F filter (Whatman) to analyze only the dissolved fraction. All samples (n = 27) were prepared to DOC quantification before and after incubation. Calculation was made according to the method in

Prijac et al. (2022). The apparent removal rate of dissolved organic carbon (RDOC), expressed in mg $day^{-1}$, corresponds to the amount of DOC removed during incubation and reported per day. Degradation rates correspond to the proportion of DOC lost per day of incubation and are expressed in %C $d^{-1}$.

### 3.4 *In situ* high frequency monitoring

According to the method described in Prijac et al. (2023) the fluorescence of DOM was measured at the drainage stream outlet at 1h interval from June 2018 to May 2020 using an EXO2 multi-parameter probe (YSI, USA). At each sampling station, water samples were analyzed for the DOC concentration and fDOM measurements taken with the EXO2 multi-parameter probe along the stream. The relationship $f$(fDOM) = [DOC], where fDOM is the corrected signal fluorescence of DOM measured in quinine sulfate units (QSU) (de Oliveira et al., 2018) and [DOC] is the dissolved organic carbon concentration in mg C $L^{-1}$, was used for DOC concentration calibration.

In addition, the stream discharge was measured using a 'V-shaped' weir installed perpendicularly to the stream. The discharge was derived from the water level in the stream measured by an ultrasonic distance sensor (SR50, Campbell, USA) during the 2018 growing season and a water-level logger (U201-04, Hobo, Onset, USA) from June 2019, to replace the ultrasonic distance sensor, damaged during the spring freshet (Prijac et al., 2023). The calculation method was described by Taillardat et al. (2022).

The DOC concentration and the stream discharge measured hourly form June 2018 to May 2020 were used to calculate the DOC exports at the stream outlet, following the calculation method described in Prijac et al. (2023).

In addition, in the wells installed in the peat, WTD was recorded hourly at the six wells (Fig. 1) equipped with a water-level data logger (HOBO, Onset, USA) for 195 continuous measurement of WTD and temperature, from June 2018 to October 2020 as described in Prijac et al. (2022). The sensors were placed into wells, suspended with a measured metal wire and kept submerged (i.e., about -0.6 m below the peat surface). Another sensor 200 was installed next to a rain gauge to record atmospheric pressure variability and to correct piezometer pressure.

### 3.5 DOC mass balance model along the stream

The stream was divided into 7 sections named *a* to *g* from upstream to the outlet according to Taillardat et al. (2022) and presented in Fig. 2.

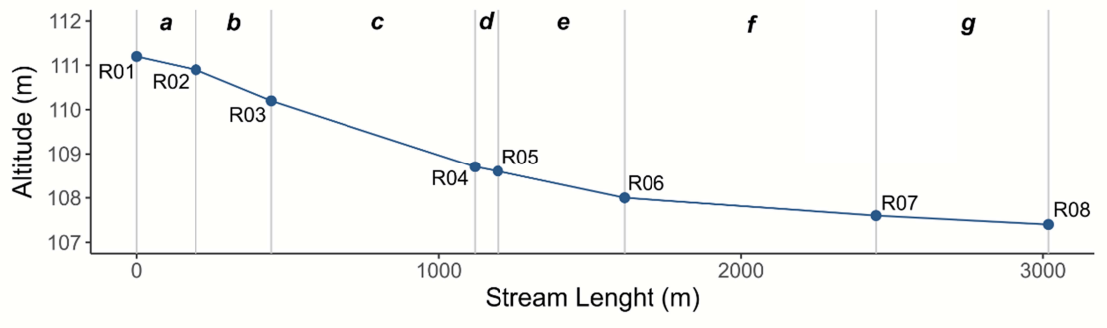


**Figure 2.** Altitude of sampling stations along the stream from the upstream sampling station (R01) to the outlet (R08). Italic letters indicate the name of sections between two sampling points.

In 2019, stream discharge was measured at each water sampling locations (Fig. 1, 2). At each section, water velocity was measured through a vertical cross-section using a portable flow velocity probe (Flow-mate model 2000, Marsh-McBirney Inc., USA) following the method described in Taillardat et al. (2022). The discharge at a station *i* ($Q_i$; $m^3\ s^{-1}$) was calculated by multiplying velocity at the station ($V_i$; $m\ s^{-1}$) by the stream section ($S_i$; $m^2$) as described in equation (1):

$$Q_i = V_i \times S_i \quad (1)$$

As a deviation was observed at the stream outlet between stream discharge measured manually and high frequency measurements measured hourly at the outlet (station R08 of figure 1), a correction was applied to punctual discharge measurements, based on the linear relation between these two discharge measurement methods ($R^2 = 0.97$). The correction is presented in equation (2) :

$$Q_{cor\,i} = 1.163 \times Q_i - 1.5637 \quad (2)$$

DOC fluxes ($fDOC_i$; g $h^{-1}$) were calculated for a station *i* by multiplying DOC concentration at the station *i* ($DOC_i$; g $m^{-3}$) by discharge at the station *i* ($Q_{cor\,i}$) (Eq. 4).

$$fDOC_i = DOC_i \times Q_{cor\,i} \quad (3)$$

The quantity of DOC that could be mineralized in the stream section ($fDOC_{min\,i}$; g $m^{-3}$) was estimated based on degradation rates of DOC measured during incubation experiments. Then estimated $fDOC_{min\,i}$ (g $m^{-3}$) was multiplied by the concentration $[DOC]_i$ (g $m^{-3}$), the degradation rates (*m*; %C $h^{-1}$) and by the water volume of the section ($V_i$; $m^3$) as presented in equation (5).

$$fDOC_{min\,i} = [DOC]_i \times m \times V_i \quad (4)$$

Then, for a section *i*, a carbon mass balance was calculated (Eq. 6 and 7). The inputs included incoming DOC from the stream ($fDOC_{i-1}$), lateral inputs of DOC in section *i* ($fDOC_{lat.inp\,i}$), and inputs of DOC from tributaries ($fDOC_{trib\,i}$). The outputs included DOC exports measured at the outlet of section *i* ($fDOC_i$) and estimated mineralization flux of DOC ($fDOC_{min\,i}$) presented in equation (4).

$$\sum fDOC_{in} = \sum fDOC_{out}$$

$$fDOC_{i-1} + fDOC_{lat.inp\,i} + fDOC_{trib\,i} = fDOC_i + fDOC_{\min i} \quad (5)$$

Based on the equation (7), lateral inputs $fDOC_{lat.inp\,i}$ can be calculated:

$$fDOC_{lat.inp\,i} = fDOC_i + fDOC_{\min i} - fDOC_{i-1} - fDOC_{trib\,i} \quad (6)$$

The proportion of $fDOC_{min}$ along the stream to fDOC measured at the outlet of the section ($\%fDOC_{min}$ ; %) was measured in order to evaluate the estimated contribution of DOC mineralization to the exported flux (Eq. 8).

$$\%fDOC_{min} = (\sum_{i=1}^{n} fDOC_{\min i})/fDOC_i \times 100 \quad (7)$$

Residence time ($r_j$; h) per stream section was calculated by dividing the length of upstream section *j* ($L_j$; m) by velocity $V_i$ ($V_i$; m $s^{-1}$) (Eq. 8):

$$r_j = L_j / V_i / 3600 \qquad (9)$$

### 3.6 Statistical analyses

Statistical tests were performed on R (CRAN-Project) through the Rstudio interface (Rstudio inc., USA) and all figures were realized with the package ggplot2 (Wickham, 2016). Data curation and statistical analysis were performed on R studio (Rstudio inc., USA), an integrated development environment of the programming langage R (CRAN-Project). Figures were realized with the package ggplot2 (Wickham, 2016).

Comparisons of variance tests were performed using the method described in Prijac et al. (2022). The mention of 'significant differences' refers to statistical tests using the following method. First, normal distribution was tested using Shapiro and Wilk test, and normal distribution was considered true when p-value was >0.05. If distribution was not normal, a Kruskal and Wallis test was performed to compare the averages and significant differences were considered true when p-value was <0.05. Dunn tests were performed as post-hoc pairwise comparison tests to determine which group was significantly different (when p-value <0.05). Second, homogeneity of variance was tested using Levene test and was considered true when p-value was >0.05. If homogeneity of variance was not true, Welsh ANOVA was performed, and significant differences were admitted when p-value was <0.05. Estimated marginal means tests were performed as post-hoc tests to determine significantly different groups (p-value <0.05). In cases where normal distribution and homogeneity of variances were true, an ANOVA was performed, and significant differences were true when p-value was <0.05. When there were significant differences, Tukey tests were performed as post-hoc tests to determine which groups were significantly different (when p-value <0.05). The statistical tests were performed between hydrological conditions in the stream and between each hydrological conditions in the stream and peat porewater for variables including DOC concentration, DOC : DON ratio, $\delta^{13}$C-DOC, $SUVA_{254}$, $E2 : E3$, $S_R$, FI and $\beta : \alpha$. The results are summarized in Table SI.1. In addition, correlation tests were performed between the variables previously mentioned and presented in correlograms for peat porewater (Fig. SI.1.a), stream (Fig. SI.1.b) and for high-flow (Fig. SI.1.c) and low-flow conditions in the stream (Fig. SI.1.d).

Linear models were performed at first between the variables including the discharge at the stream outlet ($Q_{R08}$), the proportion of $fDOC_{min}$ along the stream to the fDOC at the stream outlet ($\%fDOC_{min}$) and the total residence time in the stream (ΣRt). Linear models are summarized in Table SI.2. In a second time, linear regression was performed between the differences between the most upstream section and the outlet for the variables describing composition of DOM (Δ index) and $Q_{R08}$ (summarized in the Table SI.3.a), between Δ index and $\%fDOC_{min}$ (summarized in Table SI.3.b) and between Δ index and ΣRt (summarized in Table SI.3.c). The Δ index includes ΔDOC:DON, $\Delta SUVA_{254}$, $\Delta E2{:}E3$, $\Delta S_R$, ΔFI and $\Delta\beta{:}\alpha$.

## 4. Results

### 4.1 Experimental degradability of stream DOM

There was no significant difference between *in situ* and controlled conditions of incubation (stat = 2.66, $p$ = 0.1, Kruskal-Wallis test) and between dark conditions and natural sunlight exposition (stat = 2.96, $p$ = 0.09, Kruskal-Wallis test). This suggested a limited effect of temperature and sunlight on DOM degradation (Prijac et al., 2022).

**Table 1.** Degradation rates (% day-1) measured in the stream for *F* and UF conditions in June, August and September. *due to the low initial DOC concentration in August, no degradation rate was observed for *F* conditions

| | June | August | September |
|---|---|---|---|
| Degradation rate (% $day^{-1}$) | 3.5 ± 0.4 | * | 3.5 ± 0.4 |

Degradation rates during June and September were similar with 3.5 ± 0.4 % $day^{-1}$ both months (Table 1). In August, no degradation rates were measured and this absence of sizeable degradation can be explained by a very low initial DOC concentration of 3.1 mg $L^{-1}$. In

comparison with degradation rates in peat porewater and pools measured in Prijac et al. (2022), degradation was constantly higher in the stream for analogous incubation conditions.

### 4.2 Classification of the campaigns into low-flow and high-flow conditions

The 2019 sampling periods were classified into low-flow and high-flow conditions previously defined by a Hidden Markov model as in Prijac et al. (2023). Three sampling periods occurred during high- flow. The campaign 19B1 occurred at the end of spring freshet in June 2019. The samples from campaigns 19B3a and 19B3b correspond to sampling periods in early autumn and occurred before and after an exceptional storm. Then, three sampling periods occurred during low-flow conditions in summer (campaigns 19B2a and 19B2b) and in mid-autumn (19B4).

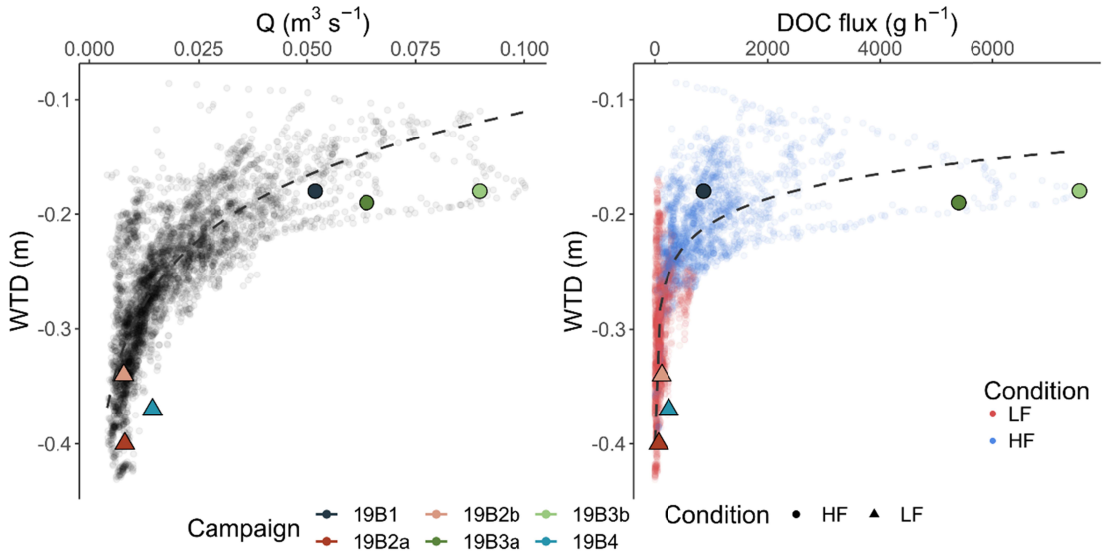


**Figure 3.** Representation of a) stream discharge at the outlet according to WTD and b) DOC flux at the outlet according to WTD measured during the six sampling periods of 2019 for WTD, Q at the stream outlet and DOC flux derived from high frequency data measurements at the study site (data from Prijac et al., 2023).

360 The classification into high and low-flow conditions allowed comparing hydrological
361 conditions and DOC exports with the full-time series from Prijac et al. (2023; Fig. 3). During the
362 campaign 19B1, DOC exports were low with 872 g $h^{-1}$ for a Q of 0.0519 $m^3$ $s^{-1}$ (Fig. 3.a). During
363 high-flow conditions, WTD varied in a narrow range from -0.18 (19B1) to -0.19 m (19B3a;
364 Table 2). Campaigns 19B3a and 19B3b corresponded to the highest DOC exports recorded with
365 values varying between $24.3\times10^{-3}$ and $33.94\times10^{-3}$ g DOC-C $m^{-2}$ $h^{-1}$ respectively with stream
366 discharge at the outlet of 0.0638 $m^3$ $s^{-1}$ during the campaign 19B3a and 0.0897 $m^3$ $s^{-1}$ during
367 campaign 19B3b (Fig 3.b).

368

**Table 2.** Values for each sampling period for WTD, discharge at the stream outlet (QR08), water temperature at the stream outlet (W.T.), fDOC at the stream outlet (fDOCR08), proportion of fDOCmin along the stream to the fDOC measured at the outlet (%fDOCmin), total retention time in the stream (ΣRt) total retention time in the stream (**Σ**Rt) and WTD.

| Campaign | Date | Condition | $Q_{R08}$ ($m^3$ $s^{-1}$) | W.T. (°C) | $fDOC_{R08}$ ($\times10^{-3}$ g DOC-C $m^{-2}$ $h^{-1}$) | $\%fDOC_{min}$ (%) | ΣRt (h) | WTD (m) |
|---|---|---|---|---|---|---|---|---|
| 19B1 | 8 June 2019 | High-flow | 0.0519 | 14.3 | 3.93 | 2.21 | 34 | -0.18 |
| 19B2a | 3 August 2019 | Low-flow | 0.0081 | 16.8 | 0.32 | 11.4 | 154 | -0.40 |
| 19B2b | 6 August 2019 | Low-flow | 0.0078 | 17.2 | 0.58[3] | 9.88 | 80 | -0.34 |
| 19B3a | 5 September 2019 | High-flow | 0.0638 | 13.8 | 24.3 | 0.98 | 13 | -0.19 |

| | | | | | | | | |
|---|---|---|---|---|---|---|---|---|
| 19B3b | 9 September 2019 | High-flow | 0.0897 | 12.8 | 33.94 | 0.93 | 18 | -0.18 |
| 19B4 | 10 October 2019 | Low-flow | 0.0144 | 8.6 | 1.14 | 5.08 | 42 | -0.37 |

For low-flow conditions, discharge at the outlet ranged from 0.0078 $m^3 s^{-1}$ (19B2b) to 0.0144 $m^3 s^{-1}$ (19B4; Fig 3.a and Table 2). During low-flow, WTD varied between -0.40 m during the campaign 19B2a and -0.34 m during the campaign 19B2b and was -0.37 m during the campaign 19B4 (Fig. 3 and Table 2). The lowest DOC exports were measured during the campaign 19B2a with 72 g $h^{-1}$ while it was 128 g $h^{-1}$ during the campaign 19B2b and 252 g $h^{-1}$ during the campaign 19B4 (Fig 3.b and Table 2).

Linear models between these indicators (*Q*, Rt and $\%fDOC_{min,}$) are summarized in the table SI.2. Negative correlations between *Q* and Rt (cor = -0.69, p-value < 0.0001) and between *Q* and $\%fDOC_{min}$ (cor = -0.59, p-value = 0.001) emerged while Rt and $\%fDOC_{min}$ were positively correlated (cor = 0.74, p-value < 0.0001). To summarize, high-flow conditions were characterized by high *Q* but shorter Rt and lower % $fDOC_{min}$, while the *Q* was lower during low-flow conditions, inducing longer Rt and higher $\%fDOC_{min}$.

### 4.3 DOM composition in peat porewater and in the stream under different hydrological conditions

DOC concentration and DOM composition differed significantly between high-flow and low-flow conditions in the stream. Contrastingly, no DOC concentration or DOM composition was significantly different in peat porewater between high-flow and low-flow conditions. Comparisons were then made between peat porewater DOM (pooling all data) and stream DOM during high-flow conditions and low-flow conditions (Fig. 4). DOC concentration increased significantly in the stream during high-flow conditions, from 9.5 ± 7.1 mg $L^{-1}$ on average during low-flow to 18.7 ± 9.6 mg $L^{-1}$ during high-flow conditions (Table 3). Significant differences

391 appeared between DOC concentration in the stream during low-flow and in peat porewater (18.0
392 ± 8.4 mg $L^{-1}$) but not during high-flow conditions (Fig. 4).

393

**Table 3.** Average (±SD) of physicochemical variables, DOC concentration, elemental ratio, isotopic ratio and optical indices in the stream (annual average and low-flow and high-flow averages) and in peat porewater (only annual average as no significant difference was found between low-flow and high-flow conditions in peat porewater).

| | Stream | | | Porewater |
|---|---|---|---|---|
| | Annual | Low-flow | High-flow | |
| Water temperature (°C) | 12.4 ± 4.3 | 11.5 ± 4.7 | 12.2 ± 3.8 | 13.4 ± 4.4 |
| pH | 4.8 ± 0.8 | 5.1 ± 0.8 | 4.5 ± 0.6 | 4.9 ± 0.7 |
| Conductivity (µS $cm^{-1}$) | 27.0 ± 12.3 | 32.0 ± 14.5 | 23.1 ± 8.6 | 32.9 ± 19.3 |
| Dissolved Oxygen (%sat) | 68.2 ± 15.4 | 65.6 ± 16.4 | 70.2 ± 14.5 | 50.0 ± 17.1 |
| DOC (mg $L^{-1}$) | 14.6 ± 9.7 | 9.5 ± 7.1 | 18.7 ± 9.6 | 18.0 ± 8.4 |
| DOC:DON ratio | 41.5 ± 17.7 | 32.5 ± 17.8 | 48.8 ± 14.1 | 48.6 ± 18.8 |
| $\delta^{13}$C-DOC (‰) | -28.1 ± 0.5 | -28.0 ± 0.6 | -28.8 ± 0.4 | -27.1 ± 0.8 |
| $SUVA_{254}$ (L $mg^{-1}$ $m^{-1}$) | 5.2 ± 1.2 | 5.8 ± 1.0 | 4.8 ± 1.1 | 5.0 ± 0.6 |
| *E*2 : *E*3 ratio | 3.7 ± 0.4 | 3.45 ± | 3.88 ± | 3.49 ± |

| | | | | |
|---|---|---|---|---|
| | | 0.46 | 0.32 | 0.17 |
| $S_R$ | 0.69 ± 0.08 | 0.65 ± 0.09 | 0.72 ± 0.06 | 0.66 ± 0.04 |
| $B : \alpha$ | 0.62 ± 0.12 | 0.69 ± 0.15 | 0.57 ± 0.06 | 0.62 ± 0.07 |
| FI | 1.34 ± 0.09 | 1.39 ± 0.10 | 1.30 ± 0.06 | 1.36 ± 0.10 |

DOC:DON ratio was significantly higher during high-flow conditions, with 48.8 ± 14.1 on average, compared to 32.5 ± 17.8 during low-flow conditions (Fig. 4.b). The average DOC:DON ratio during high-flow conditions in the stream was similar to the DOC:DON ratio in peat porewater (48.6 ± 18.8) while a significant difference was found between low-flow conditions in the stream and in peat porewater (Fig. 4.b).

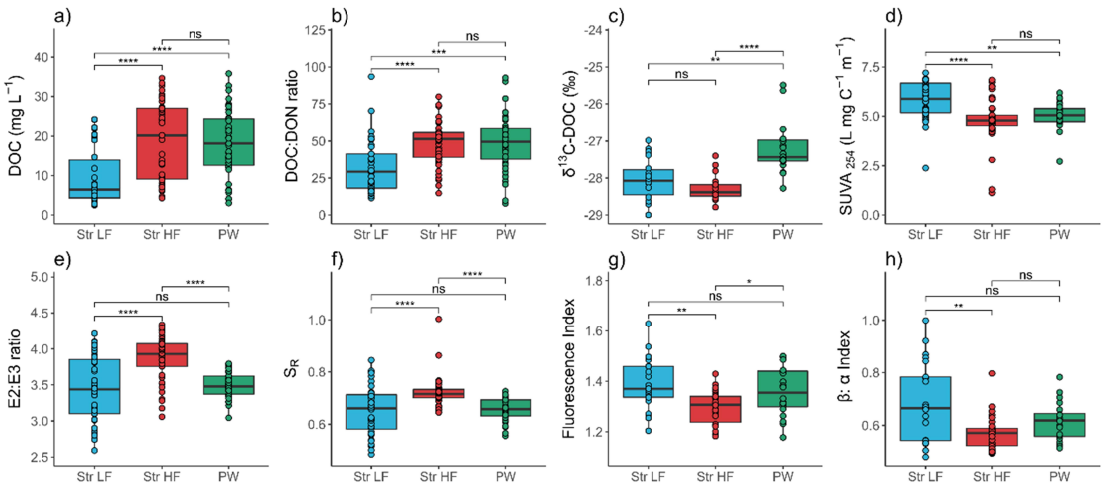


**Figure 4.** Box plots comparing values between sampling points during low-flow (Str LF) and high-flow periods in the stream (Str HF) and in peat porewater (PW) for a) DOC concentration, b) DOC:DON ratio, c) $\delta^{13}$C-DOC, d) SUVA$_{254}$, e) $E2 : E3$ ratio, f) $S_R$, g) Fluorescence index and h) $\beta : \alpha$ index. No statistical difference was found

between variables in peat porewater between high-flow and low-flow periods in the stream. The brackets indicate the significance of statistical differences between Str HF, Str LF and PW with ns: nonsignificant, * : p-values < 0.05, **: p-values < 0.01, ***: p-value < 0.001 and ****: p-value < 0.0001.

401

402 For $\delta^{13}$C-DOC, no significant difference was observed between high (-28.8 ± 0.4 ‰) and
403 low-flow (-28.0 ± 0.6 ‰; Fig. 4.c) conditions. The $\delta^{13}$C-DOC was slightly but significantly
404 lower in the stream compared to the ratio of -27.1 ± 0.8 ‰ measured in peat porewater during
405 both high- and low-flow conditions (Table 3).

406 During high-flow conditions in the stream, the $SUVA_{254}$ was significantly lower
407 compared to low-flow conditions, with 4.8 ± 1.1 L $mg^{-1}$ $m^{-1}$ and 5.8 ± 1.0 L $mg^{-1}$ $m^{-1}$ respectively
408 (Fig. 4.d). There was no significant difference between DOM aromaticity between stream during
409 high-flow and peat porewater with a $SUVA_{254}$ of 5.5 ± 0.6 L $mg^{-1}$ $m^{-1}$. The $SUVA_{254}$ in peat
410 porewater was significantly lower compared to the stream in low-flow conditions (Table 3).
411 During high-flow conditions, *E*2:*E*3 ratio was significantly higher with 3.88 ± 0.32 compared to
412 low-flow (3.45 ± 0.46 ;Fig. 4.e). The average *E*2:*E*3 ratio was significantly higher in the stream
413 during high-flow compared to peat porewater (3.5 ± 0.2) while no significant difference was
414 observed during low-flow between *E*2 : *E*3 in the stream and in peat porewater (Fig. 4.e). As for
415 *E*2 : *E*3 ratio, $S_R$ was significantly higher during high-flow conditions (0.72 ± 0.06) compared to
416 low-flow conditions (0.65 ± 0.09; Fig. 4.f). Similarly to *E*2 : *E*3 ratio, $S_R$ was slightly but
417 significantly lower in peat porewater (0.66 ± 0.04) compared to the stream during high-flow and
418 not significantly different than $S_R$ in the stream during low-flow (Table 3).

419 Fluorescence index (FI) was significantly lower during high-flow (1.30 ± 0.06) compared
420 to low-flow conditions (1.39 ± 0.10; Fig. 4.g). Also, FI was not significantly different between
421 the stream during low- flow and peat porewater (1.36 ± 0.10) while it was significantly different
422 between peat porewater and stream FI during high-flow (Fig. 4.g). The $\beta : \alpha$ index in the stream
423 during high-flow conditions was 0.57 ± 0.06 on average, and significantly lower than during
424 high-flow conditions (0.69 ± 0.15; Fig. 4.h). As for the $\beta : \alpha$ index, FI was not significantly

different between peat porewater (1.36 ± 0.10) and the stream during low-flow but significantly different during high-flow conditions (Table 3).

## 4.4 Variations in stream discharge, DOC concentration and exports, and DOM composition along the stream transect

### 4.4.1 Variations in stream discharge and DOC fluxes

Along the stream transect, discharge ranged from 0.0129 $m^3$ $s^{-1}$ (19B1) to 0.437 $m^3$ $s^{-1}$ (19B3a) at the most upstream sampling station and from 0.0519 $m^3$ $s^{-1}$ (19B1) to 0.0897 $m^3$ $s^{-1}$ (19B3b) at the stream outlet (Fig. 5.a). The most important discharge increase between the stream source to the outlet was by four times during the campaign 19B1 while it increased 1.5 times (19B3a) and 3 times (19B3b) during other campaigns.

DOC concentrations decreased during all campaigns along the stream, independently from hydrological conditions. However, during campaigns presenting the largest DOC export, the decrease was relatively limited, reaching 25.6 % during the campaign 19B3a and 13.5 % during campaing19B3b (Fig. 5.b). In comparison, two thirds of DOC was lost from upstream to downstream during 19B1 campaign. The largest decrease in DOC concentration was observed during low-flow conditions, with a decrease from 76.2 % to 87% from the most upstream section to the outlet (Fig. 5.b).

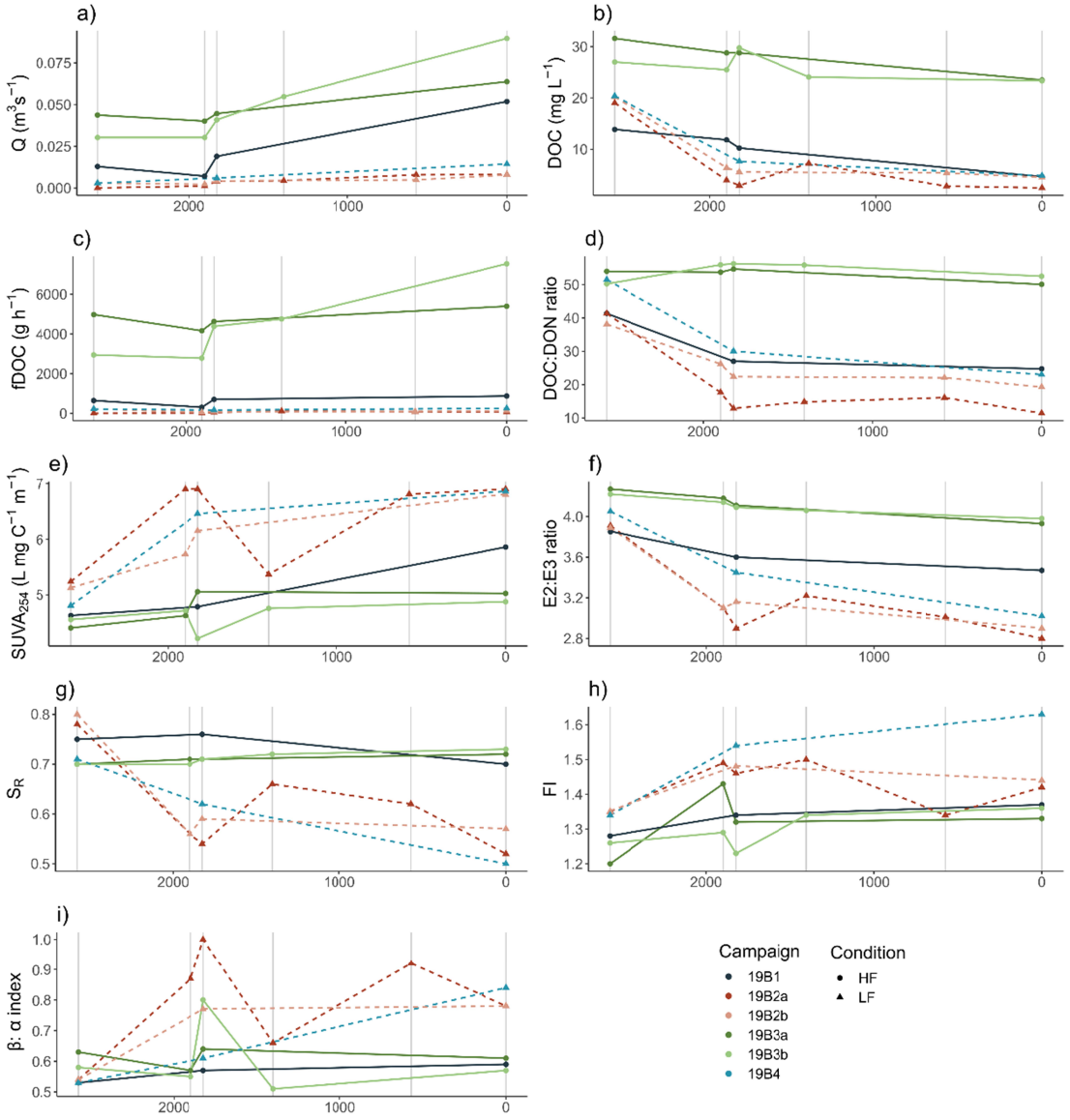


**Figure 5.** Dynamics of a) stream discharge (Q; in $m^3\ s^{-1}$), b) DOC concentration (in $mg\ L^{-1}$), c) DOC flux (fDOC; in $g\ h^{-1}$), d) DOC:DON ratio, e) $SUVA_{254}$, f) *E*2 : *E*3 ratio, g) Spectral Slope Ratio ($S_R$), h) Fluorescence Index (FI) and i) $\beta$ : $\alpha$ index according to the stream length, from the most upstream sampling station (2500 m) to the stream outlet (0 m). Points correspond to individual samples collected and grouped by campaigns in 2019.

443

DOC flux at the stream outlet ($fDOC_{R08}$) was highly variable between high- and low-flow conditions (Table 2). During most campaigns, a decrease in fDOC was observed for the most upstream section, and downstream, the fDOC constantly increased up to the stream outlet (Fig. 5.c).

### 4.4.2 Spatiotemporal evolution of DOM composition

The DOC:DON ratio remained relatively steady along the transect during high-flow conditions, except during the campaign 19B1 when ratio decreased by 53.3 % in the most upstream section and then remained relatively steady. DOC:DON decreased rapidly and intensively along the transect during low-flow conditions, with ΔDOC:DON ranging from -18.8 to -29.9 (Fig. 5.d).

The $SUVA_{254}$ constantly increased along the transect, with $\Delta SUVA_{254}$ ranging from 7% to 43% of increase. However, higher values $\Delta SUVA_{254}$ were observed during low-flow conditions (Fig. 5.e).

As for DOC:DON ratio, the highest $E2 : E3$ ratios were measured during high-flow conditions (Fig. 5.f). During all campaigns, $E2 : E3$ ratio decreased along the stream. Stronger decreases of $E2 : E3$ ratio was measured during low-flow ($\Delta E2 : E3$ ranged from -0.99 to -1.11), while $E2 : E3$ ratio decreased from -0.24 to -0.38 during high-flow conditions.

While $S_R$ values were similar between high- and low-flow conditions for the most upstream sampling station, sharper decreases were observed during low-flow conditions, with $\Delta S_R$ ranging from -0.21 to -0.26 (from -29.6 to -33.3 %). During high-flow conditions, $S_R$ fluctuated a little with $\Delta S_R$ ranging from -0.05 to 0.03. At the outlet, $S_R$ was1.2 to 1.4 times higher for high-flow conditions compared to low-flow conditions (Fig. 5.h).

The FI increased downstream during all campaigns (Fig. 5.i). Despite the fact that FI was higher during low-flow conditions compared to high-flow conditions, the increase of FI seemed not to depend on hydrological conditions, with Δ FI ranging from 0.09 to 0.13 during high-flow and Δ FI ranging from 0.07 to 0.29 during low-flow conditions.

The $\beta : \alpha$ index followed a singular pattern among indices of DOM composition. During two of six campaigns (19B2a and 19B3b), an important increase was observed in section *c* but

471 the index immediately decreased in the following section. Along the stream transect, $\beta$ : $\alpha$ index
472 increased during low-flow ($\Delta\beta$ : $\alpha$ ranged from 0.24 to 0.31), while it remained steady during
473 high-flow conditions (Fig. 5.j).

474 **4.5 Factors controlling change in DOM composition along the stream transect**

475 In general, more intense changes were observed in the stream section for low-flow
476 compared to high-flow (Fig. 6). During high-flow conditions, the DOC:DON barely did not
477 change along the stream with an average ΔDOC:DON of -2.8 ± 12.5% while it decreased by -
478 19.7 ± 20.5 % on average during low flow (Fig. 6.a). The $SUVA_{254}$ presented lower changes
479 during high-flow compared to low-flow with an average $\Delta SUVA_{254}$ of 4.2 ± 8.5% and 10.3 ±
480 16.1% for high-flow and low-flow respectively (Fig. 6.b). Indices of DOM average molecular
481 weight ($E2$:$E3$ ratio and $S_R$) showed a similar pattern with during high-flow low ($\Delta E2$:$E3$ = -2.5
482 ± 1.7%) to no changes ($\Delta S_R$ = 0.4 ± 3%) while an increase of DOM molecular weight was
483 observed during low-flow ($\Delta E2$:$E3$ = -7.4 ± 9.7%, Fig. 6.c, and $\Delta S_R$ = -8.1 ± 15.4%, Fig. 6.d).
484 For the florescence index, a more important increase was measured during low-flow (ΔFI = 4.2 ±
485 7.5%) compared to high-flow conditions (ΔFI = 2 ± 8%, Fig. 6.e). The $\beta$:$\alpha$ index also showed a
486 greater increase during low-flow conditions ($\Delta\beta$:$\alpha$ = 17.1 ± 28.9%) compared to high-flow
487 conditions ($\Delta\ \beta$:$\alpha$ = 3.4 ± 19.7%, Fig. 6.f).

488

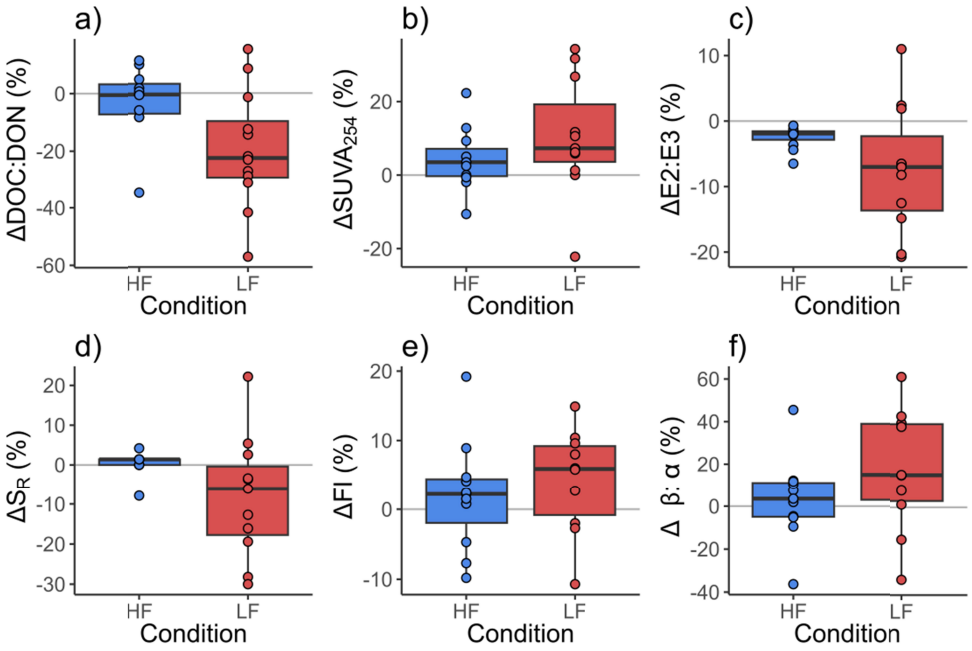


**Figure 6.** Box plots of relative change in DOM composition (in %) along the stream (from the source to the outlet) according to hydrological conditions (HF = high-flow, LF = low-flow) for a) DOC:DON ratio, b) $SUVA_{254}$, c) *E*2:*E*3 ratio, d) $S_R$, e) FI and f) *β*:*α* index.

## 5. Discussion

### 5.1 Rapid export of peat-derived DOM during high-flow conditions

During high-flow conditions, the higher average DOC concentration of 18.7 mg C $L^{-1}$ , compared to an average DOC concentration of 9.5 mg C $L^{-1}$ during low-flow conditions, suggested flushing of DOC associated with a discharge increase (Fig. 4.a; (Prijac et al., 2023). The high discharge and short residence time (Rt) during these periods (Table 2) induced only little change in DOM composition from the stream source to its outletDuring these periods, the rise of the WTD in the peat increased the hydrological connectivity between the source of DOM and the stream and led to an important mobilization of DOC within the catchment and specifically from the peatland. The composition of exported DOM presented similarities with peat porewater DOM (Fig. 4). During high-flow, high DOC : DON ratio, jointly with low

500 $SUVA_{254}$ and high $E2 : E3$ ratio was previously observed by Austnes et al. (2010) and suggested
501 the mobilization of recently produced and less biodegraded DOM.

502 Differences in composition of exported DOM and peat porewater DOM were also
503 observed through differences in average DOM molecular weight. Indices $E2 : E3$ and $S_R$ showed
504 that DOM exported through the stream during high-flow presented significantly lower molecular
505 weight compared to peat porewater (Fig. 4.e-f and Table 2). This is consistent with the
506 significant differences found between $\delta^{13}$C-DOC during high-flow conditions and in peat
507 porewater. DOM with lower molecular weight was found to be depleted in $\delta\ ^{13}$C (Guo &
508 Macdonald, 2006), consistently with the weak but significant negative correlation found in the
509 stream between $E2 : E3$ ratio and $\delta^{13}$C-DOC (cor = -0.53; $p$ = 0.035; Fig. SI. 1.b). The lowest
510 $\delta^{13}$C-DOC and $E2 : E3$ ratio supports the hypothesis that DOM exported during high-flow
511 conditions corresponds to low molecular weight molecules recently produced in the acrotelm
512 (Austnes et al., 2010) and potentially more labile (Hutchins et al., 2017).

513 **5.2 During low-flow conditions, longer residence time drives DOM processing**

514 During low-flow conditions, DOM composition was characterized by a high DOM
515 aromaticity (Fig. 5.e) and average molecular weight (Fig. 5.f-g) that increased along the stream
516 transect due to mineralization processes influenced by longer residence time. During low-flow
517 conditions, DOM composition presented characteristics of more processed DOM, reflected by
518 $SUVA_{254}$ 1.2 times higher during low-flow compared to low-flow conditions (Fig. 4.d), which is
519 known to increase with biodegradation (Autio et al., 2016; Hulatt et al., 2014; Prijac et al., 2022;
520 Saadi et al., 2006). In addition, the DOM exported during low-flow presented higher DOM
521 average molecular weight, reflected by higher $E2 : E3$ ratio and $S_R$ compared to the ones
522 measured in the stream during high-flow (Table 3) but with a similar molecular weight compared
523 to the peat porewater (Fig. 4.e-f). Higher FI and $\beta : \alpha$ index measured during low-flow conditions
524 (Fig. 4.g-h) reflected a higher proportion of microbial derived DOM (Cory et al., 2010;
525 McKnight et al., 2001; Parlanti, 2000; Wilson & Xenopoulos, 2009).

526 Similarity between isotopic ratios during low-flow and high-flow conditions ($\delta^{13}$C-DOC
527 = -28.8 ± 0.4; Table 3), suggests that the main source of DOM in the stream is the peatland as
528 low isotopic ratio is expected for peat-derived DOM (≈-28 ‰ ;Elder et al., 2000; Buzek et al.,

2019). Hence, even during low-flow conditions, peatlands are the main contributors to stream DOM in the context of peatland dominated catchment surface (Prijac et al., 2023). This is consistent with previous studies stating that wetlands and more specifically peatlands are the main source of DOM to surface water in complex catchments (Billett et al., 2006; Dick et al., 2015; Freeman et al., 2001; Rosset et al., 2019).

Contrastingly to high-flow conditions, more intense changes in DOM composition during low-flow were measured along the stream transect (Fig. 6). We hypothesize that unlike high-flow conditions, longer residence promote a shift in DOM composition along the stream. This is coherent with higher contributions of potential bio-mineralization ($\%fDOC_{min}$) measured in the stream during low-flow conditions (Table 2). The low-flow conditions, characterized by longer residence time and higher bio-mineralization, induced a high decrease in DOC:DON ratio (Fig. 6.a) and an increase in average DOM molecular weight and aromaticity, through higher average $\Delta SUVA_{254}$ (Fig. 6.b) and lower average $\Delta E2{:}E3$ (Fig. 6.c) and $\Delta S_R$ (Fig. 6.d). This is also in line with Austnes et al. (2010) who measured higher DOM aromaticity and molecular weight under low-flow conditions. Increase of DOM molecular weight during low-flow conditions is also consistent with preferential removal of low molecular weight molecules once DOM is transferred into streams (Berggren et al., 2010; Hutchins et al., 2017). This is also in accordance with the increase of DOM aromaticity observed during low-flow conditions (Fig. 5.b) that could reduce the potential biodegradability of DOM (Payandi-Rolland et al., 2020). The rapid change in DOM composition observed at our site might reflect the importance of rapid processing of allochthonous DOM in headwater streams during low-flow conditions (Hutchins et al., 2017).

### 5.3 Understanding change in DOM composition into the pulse-shunt concept

No major changes in DOM composition were observed along the stream during high-flow conditions, associated with shorter residence times (from 13 to 34h; Table 2) contrastingly to low flow conditions (Fig. 6). Based on incubation experiments, we could estimate the amount of bio-mineralized DOC in the stream ($\%fDOC_{min}$) and a positive correlation emerged between the $\%fDOC_{min}$ and $\Sigma Rt$ (Table SI.2) and a negative correlation between the $\%fDOC_{min}$ and the discharge at outlet ($Q_{R08}$; Table SI.2). These relationships and differences in DOM composition between hydrological conditions give a molecular perspective to the flux based *pulse-shunt*

concept (Raymond et al., 2016). During high-flow, the strong hydrological connectivity between the peatland and the stream favoured DOC flux but the shorter residence time reduced the contribution of DOC mineralization, down to less than 1% of fDOC at the stream outlet for the highest $Q_{R08}$ measured (Table 2). During these high-flow conditions, DOC was rapidly transferred downstream and mainly acted as a passive pipe as DOM composition was poorly impacted by bio-mineralization which was limited by shorter residence time (Casas-Ruiz et al., 2017). Contrastingly to high-flow condition, observation of important changes in DOM composition during low-flow conditions, induced by longer residence time which favored DOC mineralization in the stream, also give a new contribution to the *pulse-shunt* concept (Raymond et al., 2016). During low-flow conditions, which accounted for 44 % to 59 % of the year in the study site (Prijac et al., 2023), the headwater stream represented an active environment for DOC mineralization (Casas-Ruiz et al., 2020; Raymond et al., 2016).

DOC exports at the outlet of the stream ($fDOC_{R08}$) measured during low-flow conditions were between 3.5 and 104.6 times lower compared to fDOC at the outlet measured during high-flow conditions (Table 2). In addition, we previously observed that between 64 and 66 % of the total annual exports at the study site occurred during the top 25 % of the highest Q (Prijac et al., 2023) which tends to minor the contribution of mineralization during low-flow. Despite these low fDOC, the most important $\%fDOC_{min}$ coincided with the highest $CO_2$ exports and emissions measured at our study site during low-flow (Taillardat et al., 2022). It suggests that during low-flow, mineralization processes of exported DOM contribute, at least partially given the low fDOC, to aquatic $CO_2$ flux (Hutchins et al., 2017). Conversely, as exported DOM is rapidly transferred downstream during high-flow, aquatic $CO_2$ flux are mainly sustained by lateral transfer from the peat and emissions are stimulated by stream turbulence (Taillardat et al., 2022) rather than in-stream processing.

## 6. Conclusion

We demonstrated that DOM exported through the stream is mostly derived from the peatland but undergo important degradation processes during low-flow conditions. It supports the hypothesis that the DOC exported during high-flow conditions could specifically correspond

586 to the recently produced DOM leached from the acrotelm which is potentially labile once
587 exported in downstream to the catchment.

588 This study is the first that explores changes in DOM composition evolution along a
589 stream running through a peatland catchment and under contrasted high-flow and low-flow
590 hydrological conditions. Results reveal contrasted DOM composition dynamics between high-
591 and low-flow conditions and higher DOC concentrations during high-flow conditions. During
592 these high-flow conditions, when DOC exports were higher, DOM presented higher DOC:DON
593 ratio, lower DOM aromaticity and molecular weight, higher contributions of terrestrial-derived
594 DOM and lower contribution of microbial-derived DOM when compared to low-flow conditions.

595 In addition, greater changes in DOM composition were observed in the stream during
596 low-flow conditions, while DOM composition remained almost unchanged during high-flow. It
597 is expressed by an increase of DOM aromaticity and molecular weight with an increase of the
598 contribution of microbial-derived DOM, suggesting that these changes are induced by DOM
599 degradation. Despite the low quantity of DOC exported, the longer residence we observed during
600 these periods favored DOM microbial processing given the positive correlation between
601 retention time (Rt) and the proportion of DOC mineralization to the outlet DOC exports
602 (%$fDOC_{min}$) which supports the hypothesis that changes in DOM composition is induced by
603 instream microbial processing.

604 These results are the first to document drivers of DOM composition changes along the
605 headwater stream of a peatland dominated catchment and under different hydroclimatic
606 conditions. Our results support the important role of DOC mineralization on DOM composition
607 within the ecosystem boundaries, predominantly during low-flow, when the stream retention
608 time is longer. In the perspective of climate change, the periods of drought are expected to be
609 longer as the intensity of flood events could increase with more frequent intense rainfall events.
610 This could potentially change the balance between the exports of recently produced DOM during
611 high-flow conditions and the higher contribution of mineralization to DOM exported under low-
612 flow conditions.

## Data availability

The data have been submitted to a reliable repository and a DOI will be included in the manuscript.

## Author contributions

Conceptualisation: Laure Gandois, Michelle Garneau, Antonin Prijac and Pierre Taillardat

Data curation: Laure Gandois, Antonin Prijac and Pierre Taillardat

Data analyses: Laure Gandois, Antonin Prijac and Pierre Taillardat

Formal analyses: Laure Gandois and Antonin Prijac

Funding acquisition: Michelle Garneau

Investigation: Laure Gandois, Antonin Prijac and Pierre Taillardat

Methodology: Laure Gandois and Antonin Prijac

Data collection: Antonin Prijac and Pierre Taillardat

Writing – original draft preparation: Antonin Prijac

Writing – review and editing: Laure Gandois, Michelle Garneau, Antonin Prijac and Pierre Taillardat

## Competing interest

The authors declare that they have no conflict of interests.

## Acknowledgments

This research has been supported by the Natural Sciences and Engineering Research Council of Canada and Hydro-Québec funding to Michelle Garneau (Grant RDCPJ-51421817). We thank Katherine Velghe and Alice Parks from GRIL for their laboratory training and assistance in absorbance and fluorescence analyses, as well as Professor Paul del Giorgio for access to his laboratory. Frederic Julien, Virginie Payre-Suc, and Didier Lambrigot, from Laboratoire Ecologie Fonctionnelle et Environnement, are acknowledged for performing DOC/TN and cations/anions analyses. We thank Roman Teisserenc (Ensat, Toulouse) and Charles Bonneau,

Charles-Élie Dubé-Poirier, Camille Girard, Pénélope Germain-Chartrand, Éloïse Le Stum-Boivin, Léonie Perrier, Louis-Martin Pilote, Guillaume Primeau, Khawla Riahi, and Karelle Trottier for their assistance in the field.

## References

Austnes, K., Evans, C. D., Eliot-Laize, C., Naden, P. S., & Old, G. H. (2010). Effects of storm events on mobilisation and in-stream processing of dissolved organic matter (DOM) in a Welsh peatland catchment. *Biogeochemistry*, *99*, 157-173. https://doi.org/10.1007/s10533-009-9399-4

Autio, I., Soinne, H., Helin, J., Asmala, E., & Hoikkala, L. (2016). Effect of catchment land use and soil type on the concentration, quality, and bacterial degradation of riverine dissolved organic matter. *Ambio*, *45*(3), 331-349. https://doi.org/10.1007/s13280-015-0724-y

Berggren, M., Laudon, H., Haei, M., Ström, L., & Jansson, M. (2010). Efficient aquatic bacterial metabolism of dissolved low-molecular-weight compounds from terrestrial sources. *The ISME Journal*, *4*(3), 408-416. https://doi.org/10.1038/ismej.2009.120

Billett, M. F., Deacon, C. M., Palmer, S. M., Dawson, J. J. C., & Hope, D. (2006). Connecting organic carbon in stream water and soils in a peatland catchment. *Journal of Geophysical Research: Biogeosciences*, *111*(G2), n/a-n/a. https://doi.org/10.1029/2005JG000065

Birkel, C., Broder, T., & Biester, H. (2017). Nonlinear and threshold-dominated runoff generation controls DOC export in a small peat catchment. *Journal of Geophysical Research: Biogeosciences*, *122*(3), 498-513. https://doi.org/10.1002/2016JG003621

Bishop, K., Seibert, J., Köhler, S., & Laudon, H. (2004). Resolving the Double Paradox of rapidly mobilized old water with highly variable responses in runoff chemistry. *Hydrological Processes*, *18*(1), 185-189. https://doi.org/10.1002/hyp.5209

Broder, T., & Biester, H. (2015). Hydrologic controls on DOC, As and Pb export from a polluted peatland – the importance of heavy rain events, antecedent moisture conditions and hydrological connectivity. *Biogeosciences*, *12*(15), 4651-4664. https://doi.org/10.5194/bg-12-4651-2015

Broder, T., Knorr, K.-H., & Biester, H. (2017). Changes in dissolved organic matter quality in a peatland and forest headwater stream as a function of seasonality and hydrologic conditions. *Hydrology and Earth System Sciences*, *21*(4), 2035-2051. https://doi.org/10.5194/hess-21-2035-2017

Buzek, F., Novak, M., Cejkova, B., Jackova, I., Curik, J., Veselovsky, F., Stepanova, M., Prechova, E., & Bohdalkova, L. (2019). Assessing DOC export from a *Sphagnum* - dominated peatland using $\delta^{13}$ C and $\delta^{18}$ O–H $_2$ O stable isotopes. *Hydrological Processes*, hyp.13528. https://doi.org/10.1002/hyp.13528

673 Casas-Ruiz, J. P., Catalán, N., Gómez-Gener, L., von Schiller, D., Obrador, B., Kothawala, D.
674 N., López, P., Sabater, S., & Marcé, R. (2017). A tale of pipes and reactors : Controls on
675 the in-stream dynamics of dissolved organic matter in rivers: Controls on in-stream DOM
676 dynamics. *Limnology and Oceanography*, *62*(S1), S85-S94.
677 https://doi.org/10.1002/lno.10471

678 Casas-Ruiz, J. P., Spencer, R. G. M., Guillemette, F., Schiller, D., Obrador, B., Podgorski, D. C.,
679 Kellerman, A. M., Hartmann, J., Gómez-Gener, L., Sabater, S., & Marcé, R. (2020).
680 Delineating the Continuum of Dissolved Organic Matter in Temperate River Networks.
681 *Global Biogeochemical Cycles*, *34*(8). https://doi.org/10.1029/2019GB006495

682 Cawley, K. M., Wolski, P., Mladenov, N., & Jaffé, R. (2012). Dissolved Organic Matter
683 Biogeochemistry Along a Transect of the Okavango Delta, Botswana. *Wetlands*, *32*(3),
684 475-486. https://doi.org/10.1007/s13157-012-0281-0

685 Charman, D. (2002). *Peatlands and Environment Change* (1st Edition). Willey.

686 Cole, J. J., Prairie, Y. T., Caraco, N. F., McDowell, W. H., Tranvik, L. J., Striegl, R. G., Duarte,
687 C. M., Kortelainen, P., Downing, J. A., Middelburg, J. J., & Melack, J. (2007). Plumbing
688 the Global Carbon Cycle : Integrating Inland Waters into the Terrestrial Carbon Budget.
689 *Ecosystems*, *10*(1), 172-185. https://doi.org/10.1007/s10021-006-9013-8

690 Cory, R. M., Crump, B. C., Dobkowski, J. A., & Kling, G. W. (2013). Surface exposure to
691 sunlight stimulates $CO_2$ release from permafrost soil carbon in the Arctic. *Proceedings of*
692 *the National Academy of Sciences*, *110*(9), 3429-3434.
693 https://doi.org/10.1073/pnas.1214104110

694 Cory, R. M., McKnight, D. M., Chin, Y.-P., Miller, P., & Jaros, C. L. (2007). Chemical
695 characteristics of fulvic acids from Arctic surface waters : Microbial contributions and
696 photochemical transformations. *Journal of Geophysical Research: Biogeosciences*,
697 *112*(G4), n/a-n/a. https://doi.org/10.1029/2006JG000343

698 Cory, R. M., Miller, M. P., McKnight, D. M., Guerard, J. J., & Miller, P. L. (2010). Effect of
699 instrument-specific response on the analysis of fulvic acid fluorescence spectra :
700 Evaluating instrument-specific response. *Limnology and Oceanography: Methods*, *8*(2),
701 67-78. https://doi.org/10.4319/lom.2010.8.67

702 del Giorgio, P. A., & Pace, M. L. (2008). Relative independence of organic carbon transport and
703 processing in a large temperate river : The Hudson River as both pipe and reactor.
704 *Limnology and Oceanography*, *53*(1), 185-197. https://doi.org/10.4319/lo.2008.53.1.0185

705 de Oliveira, G., Bertone, E., Stewart, R., Awad, J., Holland, A., O'Halloran, K., & Bird, S.
706 (2018). Multi-Parameter Compensation Method for Accurate In Situ Fluorescent
707 Dissolved Organic Matter Monitoring and Properties Characterization. *Water*, *10*(9),
708 1146. https://doi.org/10.3390/w10091146

709 Dick, J. J., Tetzlaff, D., Birkel, C., & Soulsby, C. (2015). Modelling landscape controls on
710 dissolved organic carbon sources and fluxes to streams. *Biogeochemistry*, *122*(2-3),
711 361-374. https://doi.org/10.1007/s10533-014-0046-3

Dinsmore, K. J., Billett, M. F., & Dyson, K. E. (2013). Temperature and precipitation drive temporal variability in aquatic carbon and GHG concentrations and fluxes in a peatland catchment. *Global Change Biology*, *19*(7), 2133-2148. https://doi.org/10.1111/gcb.12209

Dinsmore, K. J., Billett, M. F., Skiba, U. M., Rees, R. M., Drewer, J., & Helfter, C. (2010). Role of the aquatic pathway in the carbon and greenhouse gas budgets of a peatland catchment. *Global Change Biology*, *16*(10), 2750-2762. https://doi.org/10.1111/j.1365-2486.2009.02119.x

Dubois, J. M. M. (1980). *Environments quaternaires et évolution postglaciaire d'une zone côtière en émersion en bordure sud du bouclier canadien : La moyennne Côte Nord du Saint-Laurent, Québec* [University of Ottawa]. http://dx.doi.org/10.20381/ruor-15610

Elder, J. F., Rybicki, N. B., Carter, V., & Weintraub, V. (2000). Sources and yields of dissolved carbon in northern Wisconsin stream catchments with differing amounts of peatland. *Wetlands*, *20*(1), 113-125. https://doi.org/10.1672/0277-5212(2000)020[0113:SAYODC]2.0.CO;2

Frederick, Z. A., Anderson, S. P., & Striegl, R. G. (2012). Annual estimates of water and solute export from 42 tributaries to the Yukon River. *Hydrological Processes*, *26*(13), 1949-1961. https://doi.org/10.1002/hyp.8255

Freeman, C., Evans, C. D., Monteith, D. T., Reynolds, B., & Fenner, N. (2001). Export of organic carbon from peat soils. *Nature*, *412*(6849), 785-785. https://doi.org/10.1038/35090628

Frei, S., Lischeid, G., & Fleckenstein, J. H. (2010). Effects of micro-topography on surface–subsurface exchange and runoff generation in a virtual riparian wetland—A modeling study. *Advances in Water Resources*, *33*(11), 1388-1401. https://doi.org/10.1016/j.advwatres.2010.07.006

Grand-Clement, E., Luscombe, D. J., Anderson, K., Gatis, N., Benaud, P., & Brazier, R. E. (2014). Antecedent conditions control carbon loss and downstream water quality from shallow, damaged peatlands. *Science of The Total Environment*, *493*, 961-973. https://doi.org/10.1016/j.scitotenv.2014.06.091

Guo, L., & Macdonald, R. W. (2006). Source and transport of terrigenous organic matter in the upper Yukon River : Evidence from isotope ($\delta^{13}$ C, $\Delta^{14}$ C, and $\delta^{15}$ N) composition of dissolved, colloidal, and particulate phases. *Global Biogeochemical Cycles*, *20*(2), n/a-n/a. https://doi.org/10.1029/2005GB002593

Haan, H. D., & Boer, T. D. (1987). Applicability of light absorbance and fluorescence as measures of concentration and molecular size of dissolved organic carbon in humic Lake Tjeukemeer. *Water Research*, *21*(6), 731-734. https://doi.org/10.1016/0043-1354(87)90086-8

Helms, J. R., Stubbins, A., Ritchie, J. D., Minor, E. C., Kieber, D. J., & Mopper, K. (2008). Absorption spectral slopes and slope ratios as indicators of molecular weight, source, and

photobleaching of chromophoric dissolved organic matter. *Limnology and Oceanography*, *53*(3), 955-969. https://doi.org/10.4319/lo.2008.53.3.0955

Holden, J., Smart, R. P., Dinsmore, K. J., Baird, A. J., Billett, M. F., & Chapman, P. J. (2012). Natural pipes in blanket peatlands : Major point sources for the release of carbon to the aquatic system. *Global Change Biology*, *18*(12), 3568-3580. https://doi.org/10.1111/gcb.12004

Hope, D., Billett, M. F., & Cresser, M. S. (1997). Exports of organic carbon in two river systems in NE Scotland. *Journal of Hydrology*, *193*(1-4), 61-82. https://doi.org/10.1016/S0022-1694(96)03150-2

Hulatt, C. J., Kaartokallio, H., Asmala, E., Autio, R., Stedmon, C. A., Sonninen, E., Oinonen, M., & Thomas, D. N. (2014). Bioavailability and radiocarbon age of fluvial dissolved organic matter (DOM) from a northern peatland-dominated catchment : Effect of land-use change. *Aquatic Sciences*, *76*(3), 393-404. https://doi.org/10.1007/s00027-014-0342-y

Hutchins, R. H. S., Aukes, P., Schiff, S. L., Dittmar, T., Prairie, Y. T., & del Giorgio, P. A. (2017). The Optical, Chemical, and Molecular Dissolved Organic Matter Succession Along a Boreal Soil-Stream-River Continuum. *Journal of Geophysical Research: Biogeosciences*, *122*(11), 2892-2908. https://doi.org/10.1002/2017JG004094

Kamjunke, N., Hertkorn, N., Harir, M., Schmitt-Kopplin, P., Griebler, C., Brauns, M., von Tümpling, W., Weitere, M., & Herzsprung, P. (2019). Molecular change of dissolved organic matter and patterns of bacterial activity in a stream along a land-use gradient. *Water Research*, *164*, 114919. https://doi.org/10.1016/j.watres.2019.114919

Koehler, A.-K., Sottocornola, M., & Kiely, G. (2011). How strong is the current carbon sequestration of an Atlantic blanket bog? *Global Change Biology*, *17*(1), 309-319. https://doi.org/10.1111/j.1365-2486.2010.02180.x

Lalonde, K., Middlestead, P., & Gélinas, Y. (2014). Automation of 13C 12C ratio measurement for freshwater and seawater DOC using high temperature combustion. *Limnology and Oceanography: Methods*, *12*(12), 816-829. https://doi.org/10.4319/lom.2014.12.816

Lambert, T., Teodoru, C. R., Nyoni, F. C., Bouillon, S., Darchambeau, F., Massicotte, P., & Borges, A. V. (2016). Along-stream transport and transformation of dissolved organic matter in a large tropical river. *Biogeosciences*, *13*(9), 2727-2741. https://doi.org/10.5194/bg-13-2727-2016

Lapierre, J.-F., & del Giorgio, P. A. (2014). Partial coupling and differential regulation of biologically and photochemically labile dissolved organic carbon across boreal aquatic networks. *Biogeosciences*, *11*(20), 5969-5985. https://doi.org/10.5194/bg-11-5969-2014

Laudon, H., Berggren, M., Ågren, A., Buffam, I., Bishop, K., Grabs, T., Jansson, M., & Köhler, S. (2011). Patterns and Dynamics of Dissolved Organic Carbon (DOC) in Boreal Streams : The Role of Processes, Connectivity, and Scaling. *Ecosystems*, *14*(6), 880-893. https://doi.org/10.1007/s10021-011-9452-8

789 Laurion, I., & Mladenov, N. (2013). Dissolved organic matter photolysis in Canadian arctic thaw
790 ponds. *Environmental Research Letters*, *8*(3), 035026. https://doi.org/10.1088/1748-
791 9326/8/3/035026

792 Leach, J. A., Larsson, A., Wallin, M. B., Nilsson, M. B., & Laudon, H. (2016). Twelve year
793 interannual and seasonal variability of stream carbon export from a boreal peatland
794 catchment. *Journal of Geophysical Research: Biogeosciences*, *121*(7), 1851-1866.
795 https://doi.org/10.1002/2016JG003357

796 Mann, P. J., Eglinton, T. I., McIntyre, C. P., Zimov, N., Davydova, A., Vonk, J. E., Holmes, R.
797 M., & Spencer, R. G. M. (2015). Utilization of ancient permafrost carbon in headwaters
798 of Arctic fluvial networks. *Nature Communications*, *6*(1), 7856.
799 https://doi.org/10.1038/ncomms8856

800 McKnight, D. M., Boyer, E. W., Westerhoff, P. K., Doran, P. T., Kulbe, T., & Andersen, D. T.
801 (2001). Spectrofluorometric characterization of dissolved organic matter for indication of
802 precursor organic material and aromaticity. *Limnology and Oceanography*, *46*(1), 38-48.
803 https://doi.org/10.4319/lo.2001.46.1.0038

804 Miller, M. P. (2012). The influence of reservoirs, climate, land use and hydrologic conditions on
805 loads and chemical quality of dissolved organic carbon in the Colorado River. *Water*
806 *Resources Research*, *48*(12). https://doi.org/10.1029/2012WR012312

807 Mladenov, N., McKnight, D. M., Macko, S. A., Norris, M., Cory, R. M., & Ramberg, L. (2007).
808 Chemical characterization of DOM in channels of a seasonal wetland. *Aquatic Sciences*,
809 *69*(4), 456-471. https://doi.org/10.1007/s00027-007-0905-2

810 Nilsson, M., Sagerfors, J., Buffam, I., Laudon, H., Eriksson, T., Grelle, A., Klemedtsson, L.,
811 Weslien, P., & Lindroth, A. (2008). Contemporary carbon accumulation in a boreal
812 oligotrophic minerogenic mire—A significant sink after accounting for all C-fluxes.
813 *Global Change Biology*, *14*(10), 2317-2332. https://doi.org/10.1111/j.1365-
814 2486.2008.01654.x

815 Olefeldt, D., Turetsky, M. R., & Blodau, C. (2013). Altered Composition and Microbial versus
816 UV-Mediated Degradation of Dissolved Organic Matter in Boreal Soils Following
817 Wildfire. *Ecosystems*, *16*(8), 1396-1412. https://doi.org/10.1007/s10021-013-9691-y

818 Parks, S. J., & Baker, L. A. (1997). Sources and transport of organic carbon in an Arizona river-
819 reservoir system. *Water Research*, *31*(7), 1751-1759. https://doi.org/10.1016/S0043-
820 1354(96)00404-6

821 Parlanti, E. (2000). Dissolved organic matter fuorescence spectroscopy as a tool to estimate
822 biological activity in a coastal zone submitted to anthropogenic inputs. *Organic*
823 *Geochemistry*, *31*, 1765-1781.

824 Payandi-Rolland, D., Shirokova, L. S., Tesfa, M., Bénézeth, P., Lim, A. G., Kuzmina, D.,
825 Karlsson, J., Giesler, R., & Pokrovsky, O. S. (2020). Dissolved organic matter
826 biodegradation along a hydrological continuum in permafrost peatlands. *Science of The*
827 *Total Environment*, *749*, 141463. https://doi.org/10.1016/j.scitotenv.2020.141463

828 Payette, S. (2001). Le contexte physique et biogéographique. In *Écologie des tourbières du*
829 *Québec-Labrador* (p. 9-37). Presses de l'Université Laval.

830 Prijac, A., Gandois, L., Jeanneau, L., Taillardat, P., & Garneau, M. (2022). Dissolved organic
831 matter concentration and composition discontinuity at the peat–pool interface in a boreal
832 peatland. *Biogeosciences*, *19*(18), 4571-4588. https://doi.org/10.5194/bg-19-4571-2022

833 Prijac, A., Gandois, L., Taillardat, P., Bourgault, M.-A., Riahi, K., Ponçot, A., Tremblay, A., &
834 Garneau, M. (2023). Hydrological connectivity controls dissolved organic carbon exports
835 in a peatland-dominated boreal catchment stream. *Hydrology and Earth System Sciences*,
836 *Discussions [preprint]*, 1-33. https://doi.org/10.5194/hess-2022-426

837 Primeau, G., & Garneau, M. (2021). Carbon accumulation in peatlands along a boreal to
838 subarctic transect in eastern Canada. *The Holocene*, *31*(5), 858-869.
839 https://doi.org/10.1177/0959683620988031

840 Rantakari, M., Mattsson, T., Kortelainen, P., Piirainen, S., Finér, L., & Ahtiainen, M. (2010).
841 Organic and inorganic carbon concentrations and fluxes from managed and unmanaged
842 boreal first-order catchments. *Science of The Total Environment*, *408*(7), 1649-1658.
843 https://doi.org/10.1016/j.scitotenv.2009.12.025

844 Rasilo, T., Hutchins, R. H. S., Ruiz-González, C., & del Giorgio, P. A. (2017). Transport and
845 transformation of soil-derived CO2, CH4 and DOC sustain CO2 supersaturation in small
846 boreal streams. *Science of The Total Environment*, *579*, 902-912.
847 https://doi.org/10.1016/j.scitotenv.2016.10.187

848 Raymond, P. A., Saiers, J. E., & Sobczak, W. V. (2016). Hydrological and biogeochemical
849 controls on watershed dissolved organic matter transport : Pulse-shunt concept. *Ecology*,
850 *97*(1), 5-16. https://doi.org/10.1890/14-1684.1

851 Rosset, T., Gandois, L., Le Roux, G., Teisserenc, R., Durantez Jimenez, P., Camboulive, T., &
852 Binet, S. (2019). Peatland Contribution to Stream Organic Carbon Exports From a
853 Montane Watershed. *Journal of Geophysical Research: Biogeosciences*, *124*(11),
854 3448-3464. https://doi.org/10.1029/2019JG005142

855 Roulet, N. T., Lafleur, P. M., Richard, P. J. H., Moore, T. R., Humphreys, E. R., & Bubier, J.
856 (2007). Contemporary carbon balance and late Holocene carbon accumulation in a
857 northern peatland. *Global Change Biology*, *13*(2), 397-411.
858 https://doi.org/10.1111/j.1365-2486.2006.01292.x

859 Saadi, I., Borisover, M., Armon, R., & Laor, Y. (2006). Monitoring of effluent DOM
860 biodegradation using fluorescence, UV and DOC measurements. *Chemosphere*, *63*(3),
861 530-539. https://doi.org/10.1016/j.chemosphere.2005.07.075

862 Spencer, R. G. M., Aiken, G. R., Wickland, K. P., Striegl, R. G., & Hernes, P. J. (2008).
863 Seasonal and spatial variability in dissolved organic matter quantity and composition
864 from the Yukon River basin, Alaska. *Global Biogeochemical Cycles*, *22*(4), n/a-n/a.
865 https://doi.org/10.1029/2008GB003231

Spencer, R. G. M., Mann, P. J., Dittmar, T., Eglinton, T. I., McIntyre, C., Holmes, R. M., Zimov, N., & Stubbins, A. (2015). Detecting the signature of permafrost thaw in Arctic rivers. *Geophysical Research Letters*, *42*(8), 2830-2835. https://doi.org/10.1002/2015GL063498

Stackpoole, S. M., Stets, E. G., & Striegl, R. G. (2014). The impact of climate and reservoirs on longitudinal riverine carbon fluxes from two major watersheds in the Central and Intermontane West. *Journal of Geophysical Research: Biogeosciences*, *119*(5), 848-863. https://doi.org/10.1002/2013JG002496

Taillardat, P., Bodmer, P., Deblois, C. P., Ponçot, A., Prijac, A., Riahi, K., Gandois, L., del Giorgio, P. A., Bourgault, M. A., Tremblay, A., & Garneau, M. (2022). Carbon Dioxide and Methane Dynamics in a Peatland Headwater Stream : Origins, Processes and Implications. *Journal of Geophysical Research: Biogeosciences*, *127*(7). https://doi.org/10.1029/2022JG006855

Tfaily, M. M., Hamdan, R., Corbett, J. E., Chanton, J. P., Glaser, P. H., & Cooper, W. T. (2013). Investigating dissolved organic matter decomposition in northern peatlands using complimentary analytical techniques. *Geochimica et Cosmochimica Acta*, *112*, 116-129. https://doi.org/10.1016/j.gca.2013.03.002

Tfaily, M. M., Wilson, R. M., Cooper, W. T., Kostka, J. E., Hanson, P., & Chanton, J. P. (2018). Vertical Stratification of Peat Pore Water Dissolved Organic Matter Composition in a Peat Bog in Northern Minnesota : Pore Water DOM composition in a peat bog. *Journal of Geophysical Research: Biogeosciences*, *123*(2), 479-494. https://doi.org/10.1002/2017JG004007

Tunaley, C., Tetzlaff, D., Lessels, J., & Soulsby, C. (2016). Linking high-frequency DOC dynamics to the age of connected water sources. *Water Resources Research*, *52*(7), 5232-5247. https://doi.org/10.1002/2015WR018419

Vannote, R. L., Minshall, W. G., Cummins, K. W., Sedell, J. R., & Cushing, C. E. (1980). The River Continuum Concept. *Can. J. Fish. Aquat. Sci.*, *37*(1), 130-137. https://doi.org/10.1139/f80-017

Vonk, J. E., Tank, S. E., Mann, P. J., Spencer, R. G. M., Treat, C. C., Striegl, R. G., Abbott, B. W., & Wickland, K. P. (2015). Biodegradability of dissolved organic carbon in permafrost soils and aquatic systems : A meta-analysis. *Biogeosciences*, *12*(23), 6915-6930. https://doi.org/10.5194/bg-12-6915-2015

Wallin, M. B., Grabs, T., Buffam, I., Laudon, H., Ågren, A., Öquist, M. G., & Bishop, K. (2013). Evasion of $CO_2$ from streams—The dominant component of the carbon export through the aquatic conduit in a boreal landscape. *Global Change Biology*, *19*(3), 785-797. https://doi.org/10.1111/gcb.12083

Ward, C. P., & Cory, R. M. (2016). Complete and Partial Photo-oxidation of Dissolved Organic Matter Draining Permafrost Soils. *Environmental Science & Technology*, *50*(7), 3545-3553. https://doi.org/10.1021/acs.est.5b05354

Ward, N. D., Krusche, A. V., Sawakuchi, H. O., Brito, D. C., Cunha, A. C., Moura, J. M. S., da Silva, R., Yager, P. L., Keil, R. G., & Richey, J. E. (2015). The compositional evolution of dissolved and particulate organic matter along the lower Amazon River—Óbidos to the ocean. *Marine Chemistry*, *177*, 244-256. https://doi.org/10.1016/j.marchem.2015.06.013

Weishaar, J. L., Aiken, G. R., Bergamaschi, B. A., Fram, M. S., Fujii, R., & Mopper, K. (2003). Evaluation of Specific Ultraviolet Absorbance as an Indicator of the Chemical Composition and Reactivity of Dissolved Organic Carbon. *Environmental Science & Technology*, *37*(20), 4702-4708. https://doi.org/10.1021/es030360x

Wickham, H. (2016). *Ggplot2 Elegant Graphics for Data Analysis*. Springer International Publishing. https://doi.org/10.1007/978-3-319-24277-4

Wilson, H. F., & Xenopoulos, M. A. (2009). Effects of agricultural land use on the composition of fluvial dissolved organic matter. *Nature Geoscience*, *2*(1), 37-41. https://doi.org/10.1038/ngeo391

Worrall, F., Gibson, H. S., & Burt, T. P. (2008). Production vs. Solubility in controlling runoff of DOC from peat soils – The use of an event analysis. *Journal of Hydrology*, *358*(1-2), 84-95. https://doi.org/10.1016/j.jhydrol.2008.05.037

Worrall, F., Moody, C. S., Clay, G. D., Burt, T. P., & Rose, R. (2017). The flux of organic matter through a peatland ecosystem : The role of cellulose, lignin, and their control of the ecosystem oxidation state: Flux of Organic Matter Through a Peat. *Journal of Geophysical Research: Biogeosciences*, *122*(7), 1655-1671. https://doi.org/10.1002/2016JG003697

Yamashita, Y., Scinto, L. J., Maie, N., & Jaffé, R. (2010). Dissolved Organic Matter Characteristics Across a Subtropical Wetland's Landscape : Application of Optical Properties in the Assessment of Environmental Dynamics. *Ecosystems*, *13*(7), 1006-1019. https://doi.org/10.1007/s10021-010-9370-1

Yu, Z., Loisel, J., Brosseau, D. P., Beilman, D. W., & Hunt, S. J. (2010). Global peatland dynamics since the Last Glacial Maximum. *Geophysical Research Letters*, *37*(13), n/a-n/a. https://doi.org/10.1029/2010GL043584

Zark, M., & Dittmar, T. (2018). Universal molecular structures in natural dissolved organic matter. *Nature Communications*, *9*(1), 3178. https://doi.org/10.1038/s41467-018-05665-9

Zurbrügg, R., Suter, S., Lehmann, M. F., Wehrli, B., & Senn, D. B. (2013). Organic carbon and nitrogen export from a tropical dam-impacted floodplain system. *Biogeosciences*, *10*(1), 23-38. https://doi.org/10.5194/bg-10-23-2013